Molecular dynamics simulation of nanoscale machining of copper

2003 Nanotechnology 14 390

(http://iopscience.iop.org/0957-4484/14/3/307)

INSTITUTE OF PHYSICS PUBLISHING NANOTECHNOLOGY

Nanotechnology **14** (2003) 390–396 PII: S0957-4484(03)54805-X

Molecular dynamics simulation of nanoscale machining of copper

Y Y Ye[1,2], R Biswas[1,2], J R Morris[2], A Bastawros[3] and A Chandra[4]

[1] Department of Physics and Microelectronics Research Center, Iowa State University, Ames, IA 50011, USA
[2] Ames Laboratory, Iowa State University, Ames, IA 50011, USA
[3] Department of Aerospace Engineering and Engineering Mechanics, Iowa State University, Ames, IA 50011, USA
[4] Department of Mechanical Engineering, Iowa State University, Ames, IA 50011, USA

Received 27 September 2002
Published 6 February 2003
Online at stacks.iop.org/Nano/14/390

Abstract

Molecular dynamics simulations of the nanometric cutting of single-crystal copper were performed with the embedded atom method. The nature of material removal, chip formation, material defects and frictional forces were simulated. Nanometric cutting was found to comprise two steps: material removal as the tool machines the top surface, followed by relaxation of the work material to a low defect configuration, after the tool or abrasive particle has passed over the machined region. During nanometric cutting there is a local region of higher temperature and stress below the tool, for large cutting speeds. Relaxation anneals this excess energy and leads to lower dislocation work material. At high cutting speeds (180 m s^{-1}), the machined surface is rough but the work material is dislocation free after the large excess energy has annealed the work material. At lower cutting speeds (1.8–18 m s^{-1}), the machined surface is smooth, with dislocations remaining in the substrate, and there is only a small excess temperature in the work material after machining. The size of the chip grows with increasing cutting speed.

(Some figures in this article are in colour only in the electronic version)

1. Introduction and importance of problem

There is a need to understand the fundamental atomic mechanisms underlying wear and friction between surfaces. With recent advances in nanotechnology, the wear and material removal at nanoscale dimensions involves atomic-scale properties. Magnetic hard disks involve a small nanometric separation- ($<$ 10 nm) between the rotating disk and the sliding head. Reducing wear and friction- is essential as the capacity of hard disks keeps increasing. In another application, chemical–mechanical polishing (CMP) of semiconductor substrates is a crucial state-of-the-art processing step in semiconductor technology that involves planarization of multi-level semiconductor wafers. Small abrasive particles from a slurry polish a copper surface in CMP (Steigerwald *et al* 1997). However the underlying atomic-scale processes in CMP are not fully understood.

Another leading direction in nanotechnology is the ability to create nanoscale patterns, devices and micromachines. Nano-indenters have been used to pattern atomic layers at nanometric length scales and material removal mechanisms are a critical issue. Atomic force microscopy (AFM) has probed the atomic features of sliding friction on various surfaces as a function of the load on the AFM tip (Mate *et al* 1987).

Nanoscale processing and patterning involve changes in only a few atomic layers at the surface. At such a small governing length scale, the continuum representation of the problem becomes questionable. Accordingly, a molecular dynamics (MD) based representation is sought in the present work.

2. Background of nanometric cutting simulations

There exists a body of literature on MD simulations of nanometric cutting. Various researchers (Hoover 1986, Hoover *et al* 1989, 1990, Belak and Stowers 1990, Stowers *et al* 1991, Belak 1994) have studied two- and three-dimensional

cutting of copper using the embedded atom method (EAM) (Daw and Baskes 1984, Foiles *et al* 1986) to model interatomic forces. Calculations with cutting speeds of 100 m s^{-1} with different edge radius tools and different cut depths have been reported. Belak (1994) has also investigated machining of silicon using a deformable diamond tool at a cutting speed of 540 m s^{-1} and found that a layer of atoms was transferred to the tool. The silicon in the chip and the first few layers of the newly cut surface appeared amorphous. This may be attributed to the energy requirements for transformation of the crystal into an amorphous solid being less than that required to shear the crystal.

The two-dimensional nanometric cutting of copper with a diamond tool has been simulated by Ikawa *et al* (1991), Shimada (1995) and Shimada *et al* (1991, 1993, 1994). They investigated the effect of tool-edge radius and depth of cut on the chip formation process, subsurface deformation and specific cutting energy in the [110] and [121] cutting directions. Inamura *et al* (1991, 1992, 1993, 1994) reported simulations under quasi-static conditions where only the changes in the minimum energy positions, which are the mean positions of vibrating atoms, were followed.

In a series of papers, Komanduri, Chandrasekaran and Raff (KCR) (Komanduri *et al* 2000a, 2000b, 2000c) have carried out MD simulations of nanometric cutting of single-crystal copper and aluminium. They investigated the effects of different crystal orientation, cutting direction and tool geometry on the nature of deformation and machining anisotropy of these materials. They also studied the effect of atomic scale friction in nano-scratching of single-crystal aluminium.

The nanoscale cutting by a pin tool has been studied with three-dimensional MD simulations (Fang and Weng 2000), where the frictional coefficient, and forces were determined as a function of the pin angle. Stick–slip behaviour was observed (Fang and Weng 2000). The mechanisms of wear of a diamond tool sliding on copper were simulated with MD (Zhang and Tanaka 1997) and four distinct regimes of deformation consisting of no-wear, adherence, ploughing and cutting regimes were identified. The temperature and shear distribution in nanoscale machining of copper was recently simulated (Rentsch 2000). MD simulations of a sliding copper tip on a copper surface (Sorensen *et al* 1996) found stick–slip behaviour on the (111) surface and frictional wear for other orientations.

3. Simulation method

We utilize the well established EAM, which has been very successful in modelling the elastic properties, defect formation energies and fracture mechanisms of various close-packed bulk metals (Daw and Baskes 1984, Foiles *et al* 1986). The EAM has also been widely applied to surface properties as well, successfully describing surface energies, surface reconstructions and adsorption on metal surfaces.

The basic approach of the EAM, which evolved from the density-functional theory, is that the total potential energy (U) for an atomic system is the sum of the embedding energy (F)

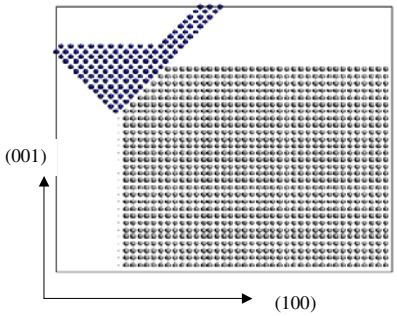

Figure 1. Initial configuration of the work material and tool with a rake angle −45°, before the nanometric cutting of the copper (100) surface. The depth of cut is 0.9 nm. The layers at the sides and bottom of the cell are rigid. An x–z plane of atoms (constant y plane) is shown.

and a short-range repulsive pair potential (ϕ) energy:

$$U = \sum_i F_i(\rho_{h,i}) + \tfrac{1}{2}\sum_{i,j}^{i\neq j} \phi_{ij}(R_{ij}). \qquad (1)$$

The embedding energy is the energy to place an atom i in a host electron density $\rho_{h,i}$ at the site of that atom. The electron density $\rho_{h,i}$ at any point is well described by a sum of the individual atomic densities. The embedding function $F(\rho_{h,i})$ incorporates quantum mechanical contributions to the cohesion of the solid. The parameters in the EAM are fitted to yield the correct lattice constants, bulk moduli and heats of formation.

Our simulation space is a work material of copper. Copper is chosen because of its importance to nanoscale processing applications and because it is an interconnect in semiconductor technology. To simulate the nanomachining of the (001) plane of copper we utilize a copper slab of dimensions $20a \times 4a \times 20a$, consisting of 6350 atoms (figure 1), where a is the lattice constant of copper (3.61 Å), similar to the workspace in previous simulations of aluminium surfaces (Komanduri *et al* 2000a). Simulations have been performed on larger systems of 15 000 atoms with similar results. The polishing is first investigated along the [100] direction of the (001) surface of copper. Periodic boundary conditions are maintained along the y direction, but not in the x or z directions. The atoms in the xz faces and the lower xy plane (bottom of the work material) are kept fixed. All other atoms are allowed to move with the MD algorithm. The predictor–corrector Gear algorithm was used for time integration of the atomic coordinates. The temperature of the entire system was maintained with a standard Nosé thermostat. Details of the workspace are summarized in table 1.

The simple scheme for the simulation of the tool consisted of initially positioning the tool at the left-hand extremity of the work material (figure 1) protruding above the surface. The tool is moved rigidly across the work material, effectively simulating the steady-state nanoscratching process. This models the mechanical abrasion and planarization of a non-uniformity on a metal surface, as may be the case in CMP.

The alternative method of indentation at various depths followed by rigid scratching of the work material produced qualitatively similar results for the nanoscale cutting to the

Table 1. Workspace and simulation parameters.

Potential for simulations	EAM	
Substrate material	Copper	
Substrate crystal structure	FCC	
Workspace dimensions 100	$20a \times 4a \times 15a$ (001) surface	6350 atoms
	$a = 3.61$ Å	(1452 atoms fixed)
Tool dimensions	$(x) \times 4a \times 11a$ (001) x depends on α_r	304 atoms
Clearance angle	45°	
Rake angle α_r	$-45°$ to $-63°$	
Cutting directions	[100] on (001) surface	
Cutting depth	$6a = 2.1$ nm (001) surface	
Cutting speed	1.8–180 m s^{-1}	
Substrate temperature	300 K	
Molecular dynamics time step	0.814 fs	

first method presented in the paper. However, it is less closely related to the steady-state machining process, and more a simulation of the initial indentation process.

The tool consists of 500–700 atoms of copper, depending on the rake angle. The (110) axis of the tool is parallel to the (100) axis of the substrate. We use indenter-like tools with negative rake angles. Since the tool width in the y direction ($3a$) is two atomic layers less than the work material it machines a channel through the work material. The tool atoms rub against the fixed atomic boundary (xz) walls of the work material. We do not allow material to pile up at the sides of the etched channel as would be expected in a full three-dimensional simulation. The simulation of a full three-dimensional nanomachining process is computationally very demanding, requiring a substantially larger unit cell, and is an aspect for further work. Key features of nanometric cutting can be described by our two-dimensional simulation geometry. The tool/abrasive is rigid and held with a downward thrust force, similar to the role of the pad in pressing abrasive particles against the surface in CMP.

The tool is displaced across the cutting surface in the [100] direction in small increments (Δx). For each position of the tool the system evolves with the MD algorithm for ∼50 time steps. The tool coordinates are then incremented along the [100] direction by Δx, and the MD simulation is repeated. As the displacement Δx is made as practically small as possible, the simulation approaches a quasicontinuous process.

In typical metal machining conditions or CMP conditions a soft copper surface is machined by a considerably harder tool or abrasive element. The hardness of diamond is 10 ℧ and abrasive alumina is 9 ℧, whereas copper is considerably softer (hardness < 5 ℧) depending on the surface preparation (Handbook of Physics and Chemistry 2002). Under such conditions it is a good approximation to consider the tool as a rigid body, which we adopt in these simulations.

The temperature is controlled by maintaining the bottom eight layers (1.2 nm) of the substrate at 300 K. Rescaling of atom velocities is performed in these lower eight layers if the temperature departs more than 10 K from the specified temperature. This algorithm allows the transfer of heat from the machined region on the surface to the bulk of the work material, similar to experiment. It is important not to rescale the atom velocities or alter the dynamics within the active machining zone. Temperature control is insensitive to small changes in the temperature tolerance.

Experimental machining of copper is performed with turning tools with machining speeds of 1–10 m s^{-1} (Shaw 1984). In semiconductor processing the rotation of the pad with rotation speeds of 20–50 RPM (Steigerwald *et al* 1997) in the CMP step produces even lower machining speeds of 0.5–1.0 m s^{-1} (Steigerwald *et al* 1997). In order to compare with this regime of machining speed we have simulated an ultra-low machining speed of 1.8 m s^{-1} by extremely small increments of $\Delta x = 0.0004$ nm. This machining speed is considerably slower than in previous simulations. Approximately 1000 displacement increments are used when the tool traverses through a distance of ∼0.4 nm. For the larger cutting speed of 18 m s^{-1}, we used $\Delta x = 0.004$ nm.

After the machining process, the work material was also allowed to relax by holding the tool in the fixed loaded position and the work material was allowed to relax through ∼150 000 time steps (120 ps). This relaxation causes reorganization of the substrate after the rapid machining step, and is essential to forming a low defect work material.

The different variables describing the nanoscale polishing process are the following.

(1) The orientation of the crystal surface and the direction of the cut.
(2) The cutting speed v_s.
(3) The depth of cut d_c.
(4) The rake angle α of the tool.
(5) The crystal orientation of the tool and the angle between the tool and work-material crystal axes.
(6) The temperature T of the substrate.
(7) The rigidity of the tool, which can be infinitely rigid or deformable.
(8) The timescale for relaxation and reorganization of the work material after the machining process.

4. Results: (001) surface machining

We first simulated the nanomachining of the (001) copper surface as a function of the cutting speed v_s, which varied from 1.8 to 180 m s^{-1}. The orientation of the cut was in the ⟨100⟩ direction. Workspace parameters shown in table 1 were employed.

Our first set of simulations with a tool with a $-45°$ rake angle displays a rich interplay between the machining speed v_s and the nature of the machined surface. Figure 2 compares results of different machining speeds after cutting

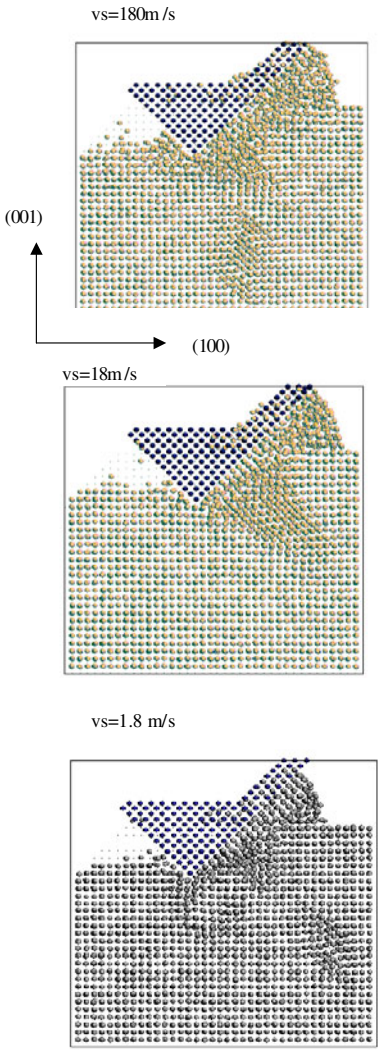

Figure 2. Final configurations after molecular dynamics simulation of the nanometric cutting of the copper (100) surface with a rigid tool with rake angle −45° at cutting speeds of 180, 18 and 1.8 m s^{-1}. The depth of cut is 1 nm in all cases.

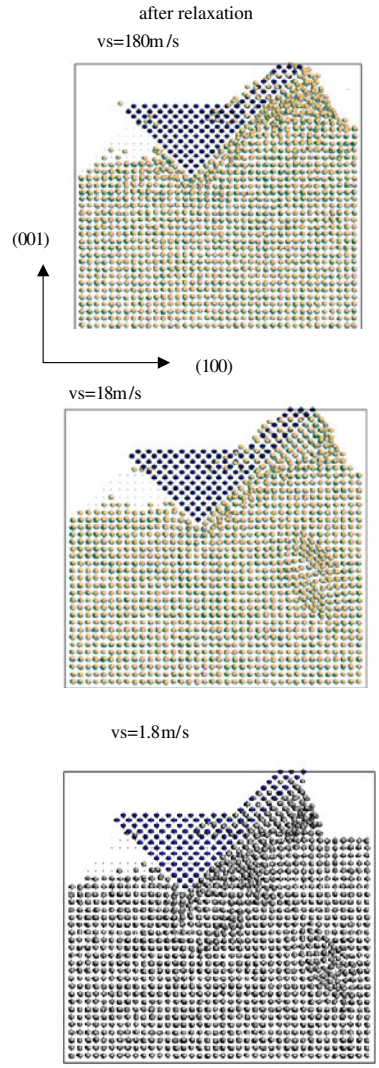

Figure 3. Configuration after the work material has relaxed with the tool in a loaded state, with an MD run of 120 ps (150 k MD steps), for the 180, 18 and 1.8 m s^{-1} cutting speeds. The final configurations shown in figure 2 were relaxed.

has progressed through ∼2.7 nm. At the highest speed (v_s = 180 m s^{-1}) the machined surface behind the tool is atomically rough, but becomes smoother as the speed decreases. There is considerable disorder and compression of the work material directly ahead of the tool for the higher speeds (180 and 18 m s^{-1}), that is reduced for v_s = 1.8 m s^{-1}. A sizable chip is formed ahead of the tool for the higher speeds (180 and 18 m s^{-1}), but is much smaller at the slowest speed (1.8 m s^{-1}), since the displaced atoms have more time to rearrange at the slower speed. Dislocations are generated for all three speeds and occur deeper in the substrate (v_s = 180 and 18 m s^{-1}, figure 2). Dislocation loops consist of pairs of missing atomic rows.

Experimentally, after the tool has traversed the machined region, there is a macroscopic time (∼ms) when the tool is away from this region and the machined surface is able to relax. We find that this relaxation step enables defects to anneal and is critical in obtaining a high quality work material.

The relaxation of the work material for 150 k MD steps (120 ps) is compared for the three machining speeds (figure 3) with the tool loaded. For v_s = 180 m s^{-1}, the compression beneath the tool and the deep dislocation loops have remarkably annealed away (figure 3), leaving behind a virtually defect-free work material. However similar dislocations remain after annealing the 18 and 1.8 m s^{-1} samples. In fact the dislocations slightly deepen during annealing of the v_s = 18 m s^{-1} sample. The disorder ahead of the tool is reduced in all cases. Behind the tool the machined surface remains rough for 180 m s^{-1} but becomes smoother as the speed is reduced to 1.8 m s^{-1}.

The remarkable relaxation for v_s = 180 m s^{-1} occurs because a high temperature region (*hot spot*) has formed beneath the tool and extends into the chip after the cutting (figure 4). Local kinetic energies beneath the tool are equivalent to temperatures of 900 K and even higher in the chip. Since the temperature locally approaches the melting temperature of Cu, substantial atomic reorganization can occur. The relaxation allows the excess energy to dissipate by heat conduction to the bulk, and anneal the highly energetic and

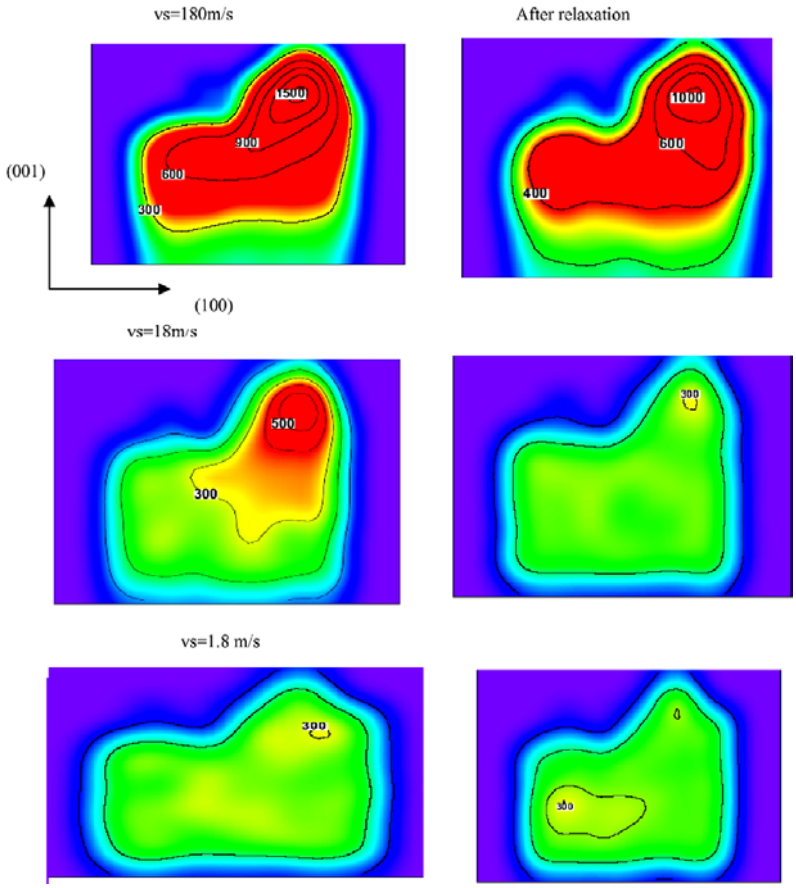

Figure 4. Spatial distribution of the local temperature (K) in the work material after the cutting simulation (configurations in figure 2), compared with the temperature after the work material was allowed to relax for 120 ps (configuration from figure 3). Pairs of results are shown for cutting speeds of 180, 18 and 1.8 m s^{-1}. The scale differs in each picture, and the values of the constant temperature contours are shown.

Table 2. Potential energies (PEs) of the work material after cutting and after relaxation.

Velocity v_s (m s^{-1})	PEs after cutting (eV/atom)	PEs after relaxation (eV/atom)
180	−3.1296	−3.2358
18	−3.2019	−3.2140
1.8	−3.2164	−3.2170

disordered atomic region. Since the temperature is very high for $v_s = 180$ m s^{-1}, the excess energy has not fully dissipated after 120 ps although considerable annealing occurs and the temperature drops to 600–1000 K in front of the tool (figure 4). Further annealing for an additional 80 ps (not shown) reduces the temperature to less than 600 K in the entire work material. In comparison, there is a much smaller temperature rise of 200 K after machining for $v_s = 18$ m s^{-1} (figure 4) that is insufficient to anneal the dislocations. There is virtually no local heating and negligible annealing during the ultra-slow 1.8 m s^{-1} simulation.

The potential energy of the work material decreases substantially by 0.1 eV/atom during annealing, due to the large structural relaxation (table 2). The potential energies for $v_s = 1.8$ and 18 m s^{-1} decrease only slightly during relaxation (table 2), consistent with the much smaller annealing for these machining speeds.

Lower speeds (18–1.8 m s^{-1}) are necessary to generate a smooth surface, whereas the higher speed (180 m s^{-1}) results in a rough surface. The dislocations at lower machining speed may be less problematic if polycrystalline substrates are used. These are the first simulations to account for the relaxation of the excess energy during nanometric cutting after the tool performs work on the substrate—a feature not simulated previously. The high temperature region below the tool suggests a build-up of stress in a local region—a feature that needs to be incorporated in continuum simulations of machining.

We have performed nanoscale machining of a considerably larger system of 12 000 atoms (figure 5) with the same orientations of the substrate and tool. The nanomachining was performed over a much larger distance of 6.8 nm. There are dislocation pairs formed beneath the tool, a disordered region in the vicinity of the tool and substantial chip formation ahead of the tool. The principal results are similar to the results on the smaller system and indicate that the smaller system can be used to describe the basic physical processes in the nanomachining process.

5. Forces on the tool and friction

We calculated the normal force or the thrust force (F_z), and the cutting force (F_x) on the tool by summing the forces from

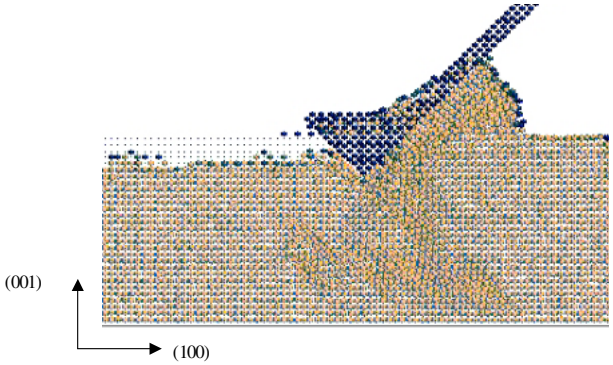

Figure 5. Nanomachining simulation of a considerably larger system with 12 000 atoms, with the surface in the (001) orientation. The configuration shown is after machining through 6.8 nm at a speed of 18 m s^{-1}.

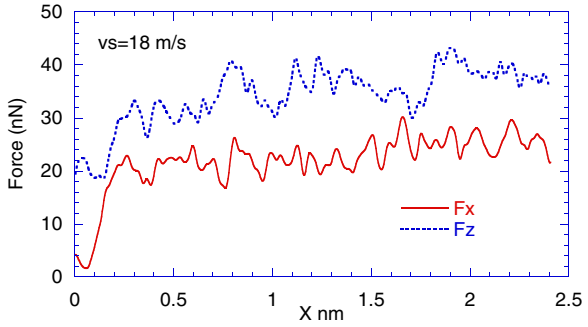

Figure 6. (a) Thrust force F_z (solid) and sliding force F_x (dashed) as the surface is machined with a tool with a rake angle of $-45°$ in the geometry of figure 2 with a speed of 18 m s^{-1}. (b) Thrust force F_z (solid) and sliding force F_x (dashed) as the surface is machined with a $-45°$ rake angle tool. There is a 45° mismatch between the crystal axis of the tool and that of the work material.

the inner layers of the tool. We neglect the force contributions of the outer layers of the tool, which rub against the work material, and are an artifact of the two-dimensional cutting geometry. Lattice registry between the work material and tool can cause large periodic variation of forces, which is avoided in this simulation. The ratio of the cutting force to the thrust force provides the coefficient of friction ($\mu = F_x/F_z$). The variation of these forces with machining distance is shown (figure 6) for the 45° tool and a 0.9 nm depth of cut and $v_s = 18$ m s^{-1}. From time-averaged forces, we obtain $\mu \cong 0.64$. A very similar variation of of forces and μ was found for the larger system in figure 5. Large values of μ may be expected for dry metal-on-metal machining where large cutting forces are generated. As the depth of cut is increased both thrust and cutting forces increase in magnitude with a qualitatively similar behaviour as in figure 6, but μ remains near this value.

Our calculated value of μ agrees well with the experimentally measured coefficients of friction (Reese 2000) for dry steel on steel of 0.6 (static coefficient) and 0.5 (kinetic coefficient). We expect the value for copper to be similar to that of steel. It is not surprising that our calculated value of μ is higher than the measured coefficient of kinetic friction since our simulation involves subsurface machining as opposed to grazing of two surfaces. The value of μ also depends on the surface smoothness.

6. Comparison with previous simulations

One critical new aspect, which we have simulated, which was not considered in previous simulations (Inamura *et al* 1993, 1994, Komanduri *et al* 2000a, 2000b, 2000c, Fang and Weng 2000), is the relaxation of the work material after the cutting has proceeded. This allows the excess energy generated in the machined region to be conducted to the bulk of the work material and is critical in annealing defects and damage. We have identified the excess energy in the machining region that can be critical in creating stresses in the work material. Excess temperatures in the work material were also found by Rentsch (2000).

The random variations in the forces when the tool and work material are mis-oriented (figure 6) are very similar to the results found by KCR. The dependence of the friction coefficient μ with crystal geometry was also found by KCR. They found values of $\mu > 1$ for tools of positive rake angle, and $\mu < 1$ for a tool with a negative rake angle of $-45°$ (Komanduri *et al* 2000a, 2000b).

Our calculated forces and calculated $\mu < 1$ agree with results found (Zhang and Tanaka 1997) for a sliding diamond asperity on the copper (111) surface in the cutting regime. Fang and Weng (2000) found the decrease of μ with the rake angle of a pin tool in three-dimensional MD simulations a result expected from continuum mechanics.

The compression of the work material below the cutting tool and formation of the chip in our simulations agrees with results of KCR (Komanduri *et al* 2000a). We have also performed simulation of cutting on the Cu(111) surface that indicates an absence of dislocations in the substrate similar to the results of KCR (Komanduri *et al* 2000a). Since the 111 surface is a natural cleavage plane, the cut surface is very flat and defect free.

It is highly encouraging that the EAM can produce results in agreement with the previous Morse-potential approaches (Komanduri *et al* 2000a, 2000b, 2000c, Fang and Weng 2000, Zhang and Tanaka 1997). This suggests that the present results are relatively insensitive to the specific interatomic potential energy function being used.

The inclusion of surface etching processes, as a result of the chemical composition of the CMP slurry, have been included in our recent simulation of nanomachining of copper (Ye *et al* 2002). The chemical etching processes are critical for achieving a planarized surface (Ye *et al* 2002).

7. Conclusions

MD simulations using the EAM have provided fundamental insight into the atomic processes underlying nanometric cutting of the single-crystal copper (001) surface. Nanometric cutting comprises of two steps: material removal as the tool machines the top surface, followed by relaxation of the work material to a low defect configuration, after the tool has passed over the machined region. During nanometric cutting there is a local region of higher temperature and stress below the tool. The relaxation process anneals this excess energy and leads to a very low dislocation work material. The material removal

observed here is similar to the mechanical part of the CMP process.

High machining speeds (180 m s^{-1}) lead to a rough machined surface with a large chip formation. There is a large increase of local kinetic energy or local temperature below the tool and in the chip. This excess energy enables the work material to relax to be virtually dislocation free. At lower machining speeds (1.8–18 m s^{-1}) there is a smooth machined surface with smaller chip formation, with dislocations remaining in the substrate. The temperature rise below the tool is much lower (<200 K) during machining. The dislocations commonly appear at 45° to the surface.

The coefficient of friction (μ) depends on the tool geometry. $\mu \sim 0.64$ for a $-45°$ rake angle tool. μ is also sensitive to the degree of orientation between the tool crystal axes and the work-material crystal axes. These MD simulations provide a new approach to controlling wear and designing a new generation of nanoscale structures.

Acknowledgments

Acknowledgement is made to the donors of the Petroleum Research Fund administered by the American Chemical Society for partial support of this research. Ames Laboratory is operated for the US Department of Energy by Iowa State University under contract No W-7405-Eng-82. We acknowledge support from the National Science Foundation through grant NSF DMI 0084736.

References

Belak J 1994 *Nanotribology: Modelling Atoms when Surfaces Collide (Energy and Technology Review)* (Livermore, CA: Lawrence Livermore Laboratory) p 13

Belak J and Stowers I F 1990 A molecular dynamics model of the orthogonal cutting process *Proc. Am. Soc. Prec. Eng.* pp 76–9

Daw M S and Baskes M I 1984 Embedded atom method: derivation and application to impurities, surfaces and other defects in metals *Phys. Rev.* B **29** 6443

Fang T and Weng C-I 2000 Three-dimensional molecular dynamics analysis of processing using a pin tool on the atomic scale *Nanotechnology* **11** 148–53

Foiles S M, Daw M S and Baskes M I 1986 Embedded atom functions for the fcc metals Cu, Ag, Au, Ni, Pd, Pt and their alloys *Phys. Rev.* B **33** 7983

Hoover W G 1986 *Molecular Dynamics (Springer Lecture Notes in Physics)* (Berlin: Springer) p 258

Hoover W G, De Groot A J, Hoover C G, Stowers I F, Kawai T, Holian B L, Boku T, Iharaa S and Belak J 1990 Large scale elastic–plastic indentation simulations via nonequilibrium molecular dynamics *Phys. Rev.* A **42** 5844

Hoover W G, Hoover C G and Stowers I F 1989 Interface tribology by nonequilibrium molecular dynamics fabrication technology *Mater Res. Soc. Symp.* **140** 119

Handbook of Physics and Chemistry 2002 (Boca Raton, FL: Chemical Rubber Company Press)

Ikawa N, Shimada S, Tanaka H and Ohmori G 1991 An atomistic analysis of nanometric chip removal as affected by tool–work interaction in diamond turning *Ann. CIRP* **40** 551

Inamura T, Suzuki H and Takezawa N 1991 Cutting experiments in a computer using atomic models of a copper crystal and a diamond tool *Int. J. Japan. Soc. Prec. Eng.* **25** 259–66

Inamura T, Takezawa N and Kumaki Y 1993 Mechanics and energy dissipation in nanoscale cutting *Ann. CIRP* **42** 79–82

Inamura T, Takezawa N, Kumaki Y and Sata T 1994 On a possible mechanism of shear deformation in nanoscale cutting *Ann. CIRP* **43** 47–50

Inamura T, Takezawa N and Taniguchi N 1992 Atomic-scale cutting in a computer using crystal models of copper and diamond *Ann. CIRP* **41** 121–4

Komanduri R, Chandrasekaran N and Raff L M 2000a Simulation of nanometric cutting of single crystal aluminum—effect of crystal orientation and direction of cutting *Wear* **242** 60–8

Komanduri R, Chandrasekaran N and Raff L M 2000b Simulation of indentation and scratching of single crystal aluminum *Wear* **242** 113–43

Komanduri R, Chandrasekaran N and Raff L M 2000c Molecular dynamics simulation of atomic-scale friction *Phys. Rev.* B **61** 14007–19

Mate C M, McClelland G W, Erlandsson R and Chiang S 1987 Atomic-scale friction of a tungsten tip on a graphite surface *Phys. Rev. Lett.* **59** 1942

Reese R L 2000 *University Physics* (New York: Brooks–Cole)

Rentsch R 2000 *Atomistic Simulation and Experimental Investigation of Ultra Precision Cutting Processes (MRS Proc. vol 578)* (Pittsburgh, PA: Materials Research Society) pp 261–6

Shaw M C (ed) 1984 *Metal Cutting Principles* (Oxford: Oxford University Press)

Shimada S 1995 Molecular dynamics analysis of nanometric cutting process *Int. J. Japan. Soc. Prec. Eng.* **29** 283–6

Shimada S, Ikawa N, Ohmori G and Tanaka H 1991 Molecular dynamics analysis as compared with experimental results of micromachining *Ann. CIRP* **41** 117

Shimada S, Ikawa N, Ohmori G, Tanaka H and Uchikoshi J 1994 Structure of micromachined surface simulated by molecular dynamics analysis *Ann. CIRP* **43** 51

Shimada S, Ikawa N, Ohmori G, Tanaka H, Uchikoshi J and Yoshinaga H 1993 Feasibility study on ultimate accuracy in microcutting using molecular dynamics simulation *Ann. CIRP* **42** 91

Sorensen M R, Jacobsen K W and Stoltze P 1996 Simulations of atomic-scale sliding friction *Phys. Rev.* B **53** 2101

Steigerwald J M, Murarka S P and Gutmann R J 1997 *Chemical Mechanical Planarization of Microelectronic Materials* (New York: Wiley)

Stowers I F, Belak J F, Lucca D A, Komanduri R, Rhorer R L, Moriwaki T, Okuda K, Ikawa H, Shimada S, Tanaka H, Dow T A and Drescher J D 1991 Molecular dynamics simulation of the chip forming process in single crystal copper and comparison with experimental data *Proc. 6th Annu. Conf. Am. Soc. Prec. Eng.* pp 100–3

Ye Y, Biswas R, Bastawros A and Chandra A 2002 Simulation of chemical mechanical planarization of copper with molecular dynamics *Appl. Phys. Lett.* **81** 1875

Zhang L and Tanaka H 1997 Towards a deeper understanding of wear and friction on the atomic scale—a molecular dynamics analysis *Wear* **211** 44–53